Electronic Supplementary Material (ESI) for Dalton Transactions.
This journal is © The Royal Society of Chemistry 2020

Supporting Information

Field-induced slow magnetic relaxation from linear trinuclear Co^{III}–Co^{II}–Co^{III} to grid [2 × 2] tetranuclear mixed-valence cobalt complexes

Meng Yang[§], Zhi-Jian Ouyang[§], Yun-Jing Zhong, Jia-Wei Cai, Xiao-Hui Li and Wen Dong*

Contents of the Supporting Information

Table S1. Crystallographic data for complexes **1**–**4**.

Table S2. Co–O and Co–N bond lengths (Å) and BVS values for Co atoms of complex **1.**

Table S3. Selected bond angles (°) for complex **1.**

Table S4. Co–O and Co–N bond lengths (Å) and BVS values for Co atoms of complex **2.**

Table S5. Selected bond angles (°) for complex **2.**

Table S6. Co–O and Co–N bond lengths (Å) and BVS values for Co atoms of complex **3.**

Table S7. Selected bond angles (°) for complex **3.**

Table S8. Co–O and Co–N bond lengths (Å) and BVS values for Co atoms of complex **4.**

Table S9. Selected bond angles (°) for complex **4.**

Table S10. SHAPE analysis for complexes **1–4**.

Fig. S1 ORTEP views (30% thermal ellipsoids) for complexes **1–4**.

Fig. S2 Structural illustrations of complex **2**.

Fig. S3 The 1D structure through the π···π stacking interaction between naphthalene rings and the 2D layer through hydrogen-bonds and the π···π stacking interaction between naphthalene rings of complex **1**.

Fig. S4 Structural illustrations of complex **4**.

Fig. S5 The 1D structure of complex **3** through the π···π stacking interaction between naphthalene rings.

Fig. S6 Powder X-ray diffraction (PXRD) patterns for complexes **1–4**.

Fig. S7 Temperature dependence of the in-phase and out-of-phase for complexes **1**–**4** at zero DC-external field.

Fig. S8 AC susceptibility data for complexes **1**–**4** at 2 K under DC applied fields in the range 0-1000 Oe.

Fig. S9 Frequency dependence of the in-phase components for the ac magnetic susceptibility in a 1 kOe dc field for complexes **1** and **2**.

Fig. S10 Frequency dependence of the in-phase components for the ac magnetic susceptibility in a 1 kOe dc field for complexes **3** and **4**.

Fig. S11 Cole−Cole plots for complex **2**.

Table S1. Crystallographic data for complexes **1**–**4**.

Complex	**1**	**2**	**3**	**4**
Formula	$C_{60}H_{74}Co_3N_{28}O_{19}$	$C_{56}H_{60}Co_3N_{28}O_{16}$	$C_{134}H_{138}Co_6N_{66}O_{32}$	$C_{130}H_{134}Co_6N_{58}O_{30}S_8$
Formula weight	1668.26	1558.11	3538.68	3599.01
T (K)	100.00(10)	120(2)	100.0(4)	100(10)
Crystal system	Monoclinic	Triclinic	Triclinic	Triclinic
Space group	$P2_1/n$	$P\bar{1}$	$P\bar{1}$	$P\bar{1}$
a (Å)	12.46890(10)	9.3778(9)	15.3105(3)	14.8320(3)
b (Å)	14.21320(10)	12.6936(11)	15.6182(3)	16.1866(3)
c (Å)	19.8528(2)	13.7782(13)	16.7603(4)	16.9537(4)
α (deg)	90	89.076(4)	91.460(2)	93.051(2)
β (deg)	95.6180(10)	83.116(4)	105.601(2)	104.841(2)
γ (deg)	90	81.505(4)	101.919(2)	103.502(2)
θ/ (deg)	3.831–76.996	2.51–27.584	2.223–27.5	2.716–76.925
V(Å^3)	3501.47(5)	1610.4(3)	3762.90(14)	3797.95(15)
Z	2	1	1	1
D_c (g·cm^{-3})	1.582	1.607	1.562	1.574
μ (mm^{-1})	6.298	0.856	0.745	6.822
Unique reflns, R_{int}	7119/0.0356	7458/0.0570	17106/0.0618	15400/0.0501
GOF	1.041	1.054	1.036	1.031
$R_1(I > 2\sigma(I))$	0.0446	0.0347	0.0437	0.0856
wR_2 ($I > 2\sigma(I)$)	0.1206	0.0817	0.1020	0.2157
R_1(all data)	0.0482	0.0447	0.0698	0.0942
wR_2 (all data)	0.1230	0.0857	0.1117	0.2226

Table S2. Co–O and Co–N bond lengths (Å) and BVS values for Co atoms of complex **1.**

Complex **1**			
Bond	Bond Length / Å	Bond Valence calculated by Co^{II}–N/O R_0 parameters	Bond Valence calculated by Co^{III}–N/O R_0 parameters
Co(1)–O(1)	2.0883(16)	0.336	0.295
Co(1)–O(1′)	2.0883(16)	0.336	0.295
Co(1)–O(2)	2.1139(18)	0.314	0.275
Co(1)–O(2′)	2.1139(18)	0.314	0.275
Co(1)–N(1)	2.1221(19)	0.337	0.311
Co(1)–N(1′)	2.1221(19)	0.337	0.311
		∑v(Co^{II}) = 1.974	**∑v(Co^{III}) = 1.762**
Co(2)–O(3)	1.8986(17)	0.561	0.493
Co(2)–O(4)	1.9171(2)	0.534	0.469
Co(2)–N(2)	1.901(2)	0.613	0.565
Co(2)–N(3)	1.888(2)	0.635	0.584
Co(2)–N(4)	1.896(2)	0.621	0.573
Co(2)–N(5)	1.895(2)	0.623	0.575
		∑v(Co^{II}) = 3.587	**∑v(Co^{III}) = 3.259**

Bond Valence = $\exp[(R_0-d_{ij})/b]$, R_0 = 1.685 for Co^{II}–O, 1.720 for Co^{II}–N, 1.637 for Co^{III}–O and 1.690 for Co^{III}–N, b = 0.37.[1]

Table S3. Selected bond angles (°) for complex **1.**

Complex **1**			
Bond	Angle / °	Bond	Angle / °
O(1)–Co(1)–O(2)	90.54(7)	O(1)–Co(1)–N(1)	88.40(7)
O(2)–Co(1)–N(1)	90.75(7)	O(3)–Co(2)–O(4)	90.05(8)
O(3)–Co(2)–N(2)	164.91(8)	O(4)–Co(2)–N(2)	89.37(8)
O(3)–Co(2)–N(3)	84.72(8)	O(4)–Co(2)–N(3)	99.67(8)
N(2)–Co(2)–N(3)	80.52(8)	N(3)–Co(2)–N(5)	95.32(8)
N(3)–Co(2)–N(4)	176.08(8)	O(3)–Co(2)–N(5)	90.32(8)
O(4)–Co(2)–N(5)	164.97(8)	N(4)–Co(2)–N(5)	80.77(8)
O(3)–Co(2)–N(4)	95.53(8)	O(4)–Co(2)–N(4)	84.24(8)
N(2)–Co(2)–N(4)	99.41(8)	N(2)–Co(2)–N(5)	94.12(8)

Table S4. Co–O and Co–N bond lengths (Å) and BVS values for Co atoms of complex **2.**

Complex **2**			
Bond	Bond Length / Å	Bond Valence calculated by Co^{II}–N/O R_0 parameters	Bond Valence calculated by Co^{III}–N/O R_0 parameters
Co(1)–O(1)	2.1058(14)	0.321	0.282
Co(1)–O(1′)	2.1058(14)	0.321	0.282
Co(1)–O(2)	2.1154(15)	0.312	0.274
Co(1)–O(2′)	2.1154(15)	0.312	0.274
Co(1)–N(1)	2.1105(16)	0.348	0.321
Co(1)–N(1′)	2.1105(16)	0.348	0.321
		∑v(Co^{II}) = 1.962	**∑v(Co^{III}) = 1.754**
Co(2)–O(3)	1.8988(13)	0.561	0.493
Co(2)–O(4)	1.8881(13)	0.577	0.507
Co(2)–N(2)	1.8823(15)	0.645	0.595
Co(2)–N(3)	1.8992(16)	0.616	0.568
Co(2)–N(4)	1.8851(15)	0.640	0.590
Co(2)–N(5)	1.9028(16)	0.610	0.563
		∑v(Co^{II}) = 3.649	**∑v(Co^{III}) = 3.316**

Bond Valence = $\exp[(R_0-d_{ij})/b]$, R_0 = 1.685 for Co^{II}–O, 1.720 for Co^{II}–N, 1.637 for Co^{III}–O and 1.690 for Co^{III}–N, b = 0.37.[1]

Table S5. Selected bond angles (°) for complex **2.**

Complex **2**			
Bond	Angle / °	Bond	Angle / °
O(1)-Co(1)-O(2)	92.69(6)	O(1)-Co(1)-N(1)	94.57(6)
O(2)-Co(1)-N(1)	90.68(6)	O(3)-Co(2)-O(4)	88.98(6)
O(3)-Co(2)-N(2)	85.15(6)	O(3)-Co(2)-N(3)	165.97(6)
O(3)-Co(2)-N(4)	92.23(6)	O(3)-Co(2)-N(5)	93.13(6)
O(4)-Co(2)-N(2)	93.65(6)	O(4)-Co(2)-N(3)	90.34 (6)
O(4)-Co(2)-N(4)	85.48(6)	O(4)-Co(2)-N(5)	166.50(6)
N(2)-Co(2)-N(3)	80.90(7)	N(2)-Co(2)-N(4)	177.26(7)
N(2)-Co(2)-N(5)	99.81(7)	N(3)-Co(2)-N(4)	101.69(7)
N(3)-Co(2)-N(5)	90.80(7)	N(4)-Co(2)-N(5)	81.12(7)

Table S6. Co–O and Co–N bond lengths (Å) and BVS values for Co atoms of complex **3.**

Complex **3**

Bond	Bond Length / Å	Bond Valence calculated by Co^{II}–N/O R_0 parameters	Bond Valence calculated by Co^{III}–N/O R_0 parameters
Co(1)–O(1)	1.8915(16)	0.572	0.503
Co(1)–O(3)	1.8935(17)	0.569	0.500
Co(1)–N(1)	1.9118(19)	0.595	0.549
Co(1)–N(6)	1.8870(19)	0.637	0.587
Co(1)–N(7)	1.908(2)	0.602	0.555
Co(1)–N(12)	1.8898(19)	0.632	0.599
		∑v(Co^{II}) = 3.607	**∑v(Co^{III}) = 3.293**
Co(2)–O(5)	2.0955(17)	0.330	0.290
Co(2)–N(3^1)	2.155(2)	0.309	0.285
Co(2)–N(10)	2.0875(19)	0.370	0.341
Co(2)–N(13)	2.168(2)	0.298	0.275
Co(2)–N(15)	2.089(2)	0.369	0.340
Co(2)–N(17)	2.147(2)	0.315	0.291
		∑v(Co^{II}) = 1.991	**∑v(Co^{III}) = 1.822**
Co(3)–O(6)	1.8843(17)	0.584	0.513
Co(3)–O(8)	1.8918(17)	0.572	0.502
Co(3)–N(18)	1.915(2)	0.590	0.544
Co(3)–N(23)	1.902(2)	0.611	0.564
Co(3)–N(24)	1.900(2)	0.615	0.567
Co(3)–N(29)	1.8975(19)	0.619	0.571
		∑v(Co^{II}) = 3.591	**∑v(Co^{III}) = 3.261**

Bond Valence = $\exp[(R_0-d_{ij})/b]$, R_0 = 1.685 for Co^{II}–O, 1.720 for Co^{II}–N, 1.637 for Co^{III}–O and 1.690 for Co^{III}–N, b = 0.37.[1]

Table S7. Selected bond angles (°) for complex **3.**

Complex **3**			
Bond	Angle / °	Bond	Angle / °
O3–Co1–N7	165.74(7)	N6–Co1–N7	101.70(8)
O3–Co1–N1	89.32(8)	N6–Co1–N12	177.67(9)
O1–Co1–O3	90.90(7)	N6–Co1–N1	80.76(8)
O1–Co1–N7	90.44(8)	N12–Co1–O3	85.20(8)
O1–Co1–N1	165.87(8)	N12–Co1–O1	94.29(8)
N7–Co1–N1	92.82(8)	N12–Co1–N7	80.55(8)
N6–Co1–O3	92.56(8)	N12–Co1–N1	99.81(8)
N6–Co1–O1	85.12(8)	O5–Co2–N13	85.95(7)
O5–Co2–N3[1]	169.53(7)	N15–Co2–O5	98.26(7)
O5–Co2–N17	91.53(7)	N15–Co2–N13	74.72(7)
N10–Co2–O5	85.00(7)	N15–Co2–N3[1]	84.66(7)
N10–Co2–N15	176.70(8)	N15–Co2–N17	74.89(8)
N10–Co2–N13	106.14(7)	N3[1]–Co2–N13	85.13(8)
N10–Co2–N3[1]	92.22(8)	N17–Co2–N13	148.80(8)
N10–Co2–N17	104.60(8)	N17–Co2–N3[1]	98.94(8)
O8–Co3–N29	84.92(8)	O6–Co3–N23	84.85(8)
O8–Co3–N24	165.06(8)	N29–Co3–N24	80.52(9)
O8–Co3–N18	89.87(8)	N29–Co3–N18	106.58(8)
O8–Co3–N23	92.95(8)	N29–Co3–N23	172.67(9)
O6–Co3–O8	91.57(7)	N24–Co3–N18	91.09(9)
O6–Co3–N29	88.19(8)	N24–Co3–N23	101.91(8)
O6–Co3–N24	91.30(8)	N23–Co3–N18	80.39(8)
O6–Co3–N18	165.23(8)		

1: 1-x,1-y,1-z

Table S8. Co–O and Co–N bond lengths (Å) and BVS values for Co atoms of complex **4.**

Complex **4**

Bond	Bond Length / Å	Bond Valence calculated by Co^{II}–N/O R_0 parameters	Bond Valence calculated by Co^{III}–N/O R_0 parameters
Co(1)–O(2)	1.897(3)	0.564	0.495
Co(1)–O(3)	1.895(4)	0.567	0.498
Co(1)–N(1)	1.913(4)	0.594	0.547
Co(1)–N(6)	1.899(4)	0.616	0.568
Co(1)–N(7)	1.905(4)	0.606	0.559
Co(1)–N(12)	1.907(4)	0.603	0.556
		$\sum v(Co^{II}) = 3.550$	**$\sum v(Co^{III}) = 3.223$**
Co(2)–O(14)	2.609(2)	0.348	0.306
Co(2)–N(15)	2.204(3)	0.267	0.246
Co(2)–N(22)	2.066(2)	0.391	0.361
Co(2)–N(25)	2.167(3)	0.299	0.299
Co(2)–N(27)	2.072(3)	0.388	0.358
Co(2)–N(29)	2.142(3)	0.322	0.275
		$\sum v(Co^{II}) = 2.017$	**$\sum v(Co^{III}) = 1.845$**
Co(3)–O(5)	1.899(2)	0.563	0.494
Co(3)–O(7)	1.893(2)	0.571	0.502
Co(3)–N(13)	1.919(3)	0.599	0.544
Co(3)–N(18)	1.896 (3)	0.603	0.558
Co(3)–N(19)	1.902(3)	0.605	0.556
Co(3)–N(24)	1.890(3)	0.611	0.564
		$\sum v(Co^{II}) = 3.543$	**$\sum v(Co^{III}) = 3.218$**

Bond Valence = $\exp[(R_0-d_{ij})/b]$, R_0 = 1.685 for Co^{II}–O, 1.720 for Co^{II}–N, 1.637 for Co^{III}–O and 1.690 for Co^{III}–N, b = 0.37.[1]

Table S9. Selected bond angles (°) for complex **4.**

Complex **4**			
Bond	Angle / °	Bond	Angle / °
O(2)–Co(1)–O(3)	93.32(15)	O(2)–Co(1)–N(1)	165.10(17)
O(2)–Co(1)–N(6)	84.77(16)	O(2)–Co(1)–N(7)	89.51(16)
O(2)–Co(1)–N(12)	91.73(16)	O(3)–Co(1)–N(1)	89.59(17)
O(3)–Co(1)–N(6)	90.74(16)	O(3)–Co(1)–N(7)	164.94(17)
O(3)–Co(1)–N(12)	84.78(17)	N(1)–Co(1)–N(6)	80.58(17)
N(1)–Co(1)–N(7)	91.48(18)	N(1)–Co(1)–N(12)	103.09(18)
N(6)–Co(1)–N(7)	104.25(18)	N(6)–Co(1)–N(12)	174.15(18)
N(7)–Co(1)–N(12)	80.35(18)	O(14)–Co(2)–N(15A)	170.85(17)
O(14)–Co(2)–N(22)	90.21(16)	O(14)–Co(2)–N(25)	87.21(17)
O(14)–Co(2)–N(27)	92.32(17)	O(14)–Co(2)–N(29)	92.38(17)
N(15A)–Co(2)–N(22)	89.43(16)	N(15A)–Co(2)–N(25)	84.11(16)
N(15A)–Co(2)–N(27)	88.28(16)	N(15A)–Co(2)–N(29)	102.80(17)
N(22)–Co(2)–N(25)	106.23(17)	N(22)–Co(2)–N(27)	177.15(17)
N(22)–Co(2)–N(29)	102.80(17)	N(25)–Co(2)–N(27)	75.20(17)
O(5)–Co(3)–O(7)	90.58(15)	O(5)–Co(3)–N(13)	90.26(16)
O(5)–Co(3)–N(18)	94.38(16)	O(5)–Co(3)–N(19)	165.62(16)
O(5)–Co(3)–N(24)	84.76(16)	O(7)–Co(3)–N(13)	166.08(15)
O(7)–Co(3)–N(18)	85.10(15)	O(7)–Co(3)–N(19)	88.78(16)
O(7)–Co(3)–N(24)	94.62(16)	N(13)–Co(3)–N(18)	80.99(16)
N(13)–Co(3)–N(19)	93.80(17)	N(13)–Co(3)–N(24)	99.29(17)
N(18)–Co(3)–N(19)	99.87(17)	N(18)–Co(3)–N(24)	179.09(17)
N(19)–Co(3)–N(24)	80.98(17)		

A: 1-x,1-y,1-z

Table S10. SHAPE analysis for complexes **1**–**4**.

complex	HP-6	PPY-6	OC-6	TPR-6	JPPY-6
1	32.632	29.967	**0.022**	16.408	33.428
2	30.291	28.925	**0.145**	16.089	32.228
3	32.224	21.994	**2.333**	10.128	25.651
4	33.515	24.279	**1.794**	11.506	28.003

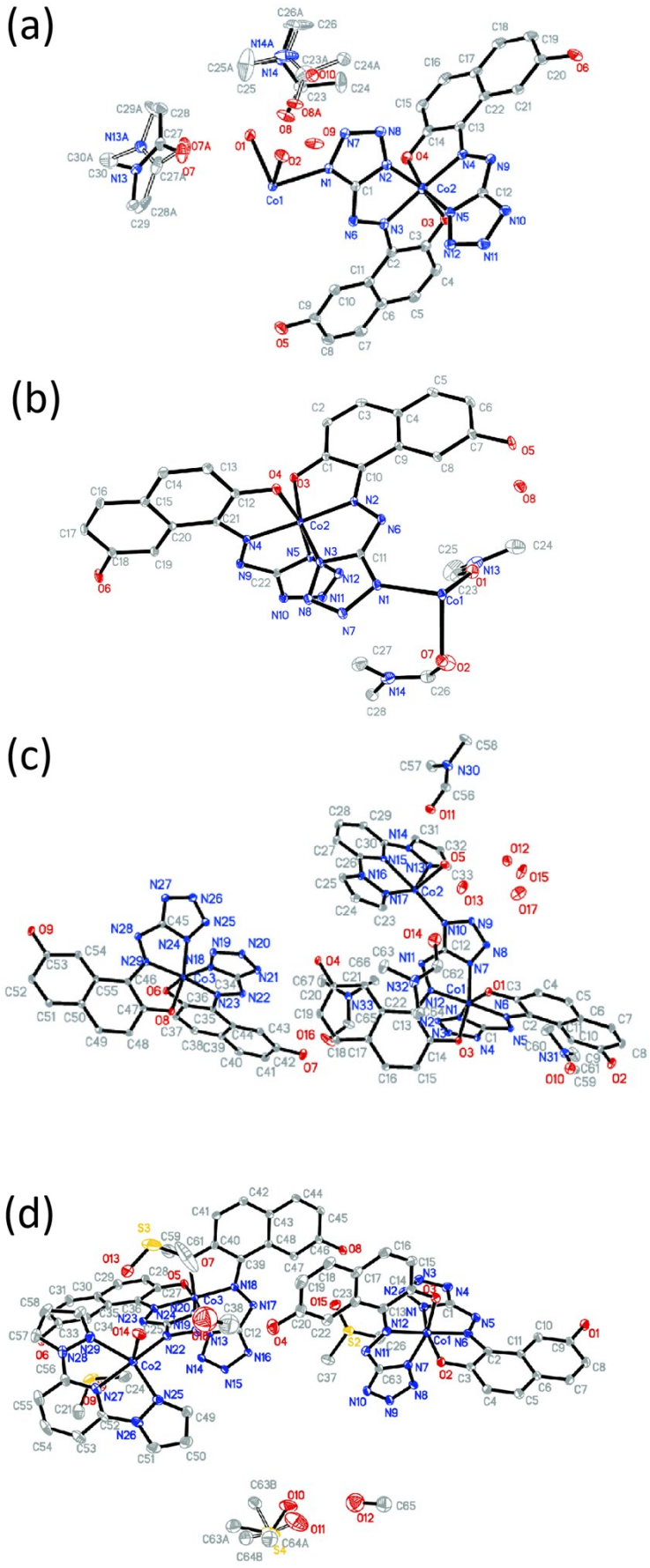

Fig. S1 ORTEP views (30% thermal ellipsoids) for complexes **1**(a)**, 2**(b)**, 3**(c) and **4**(d)**.**

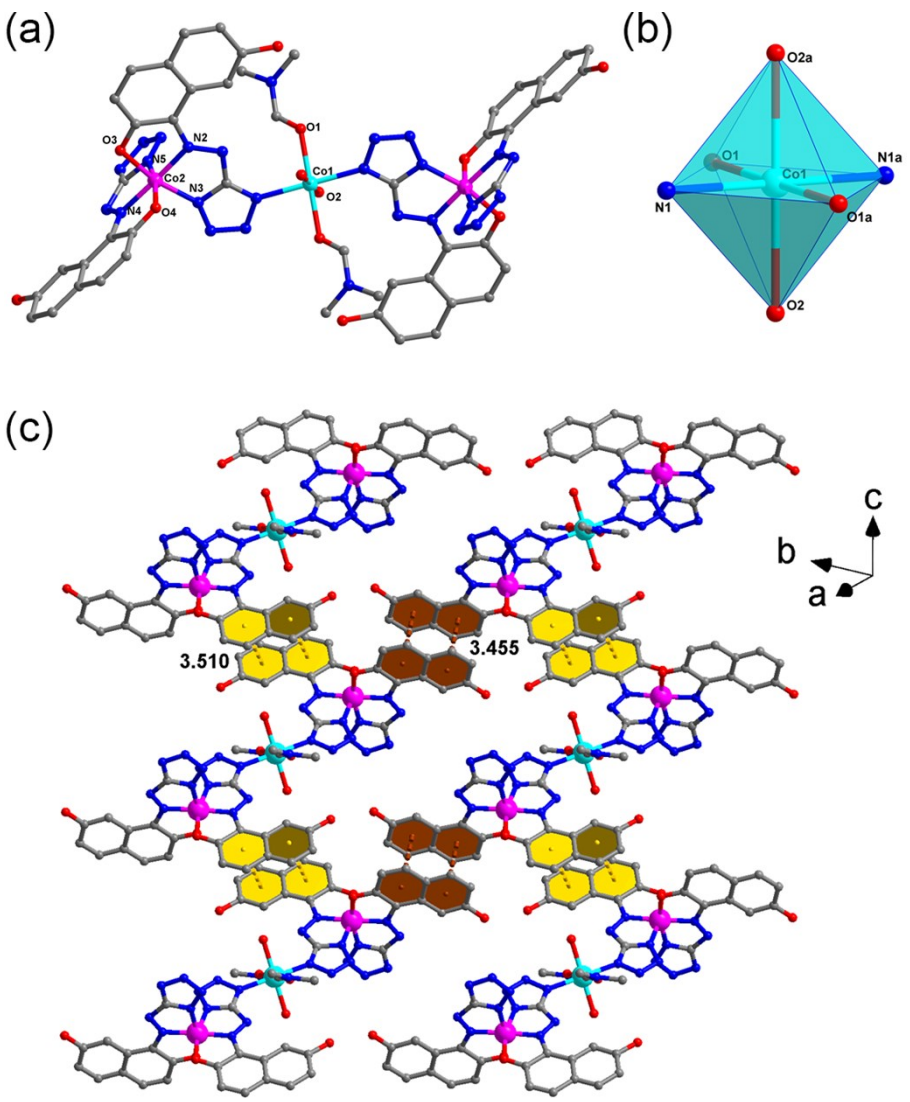

Fig. S2 Structural illustrations of complex **2**: Coordination environments of Co1 and Co2 (a); Local coordination geometry of Co1 (b) and 2D structure through the π···π stacking interaction between naphthalene rings (c). Color code: pink, Co^{III}; turquoise, Co^{II}; gray, C; blue, N; red, O. Hydrogen atoms and uncoordinated solvent molecules were omitted for clarity reason.

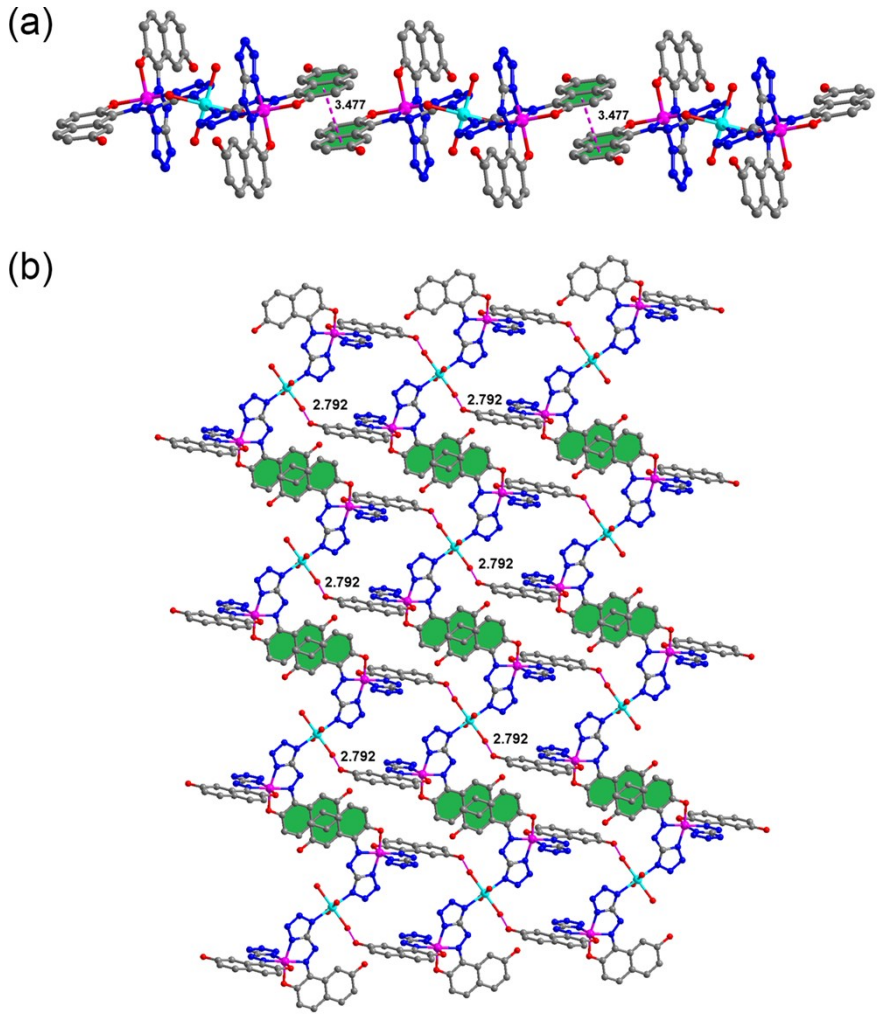

Fig. S3 The 1D structure through the π···π stacking interaction between naphthalene rings (a) and the 2D layer through hydrogen-bonds and the π···π stacking interaction between naphthalene rings (b) of complex **1**.

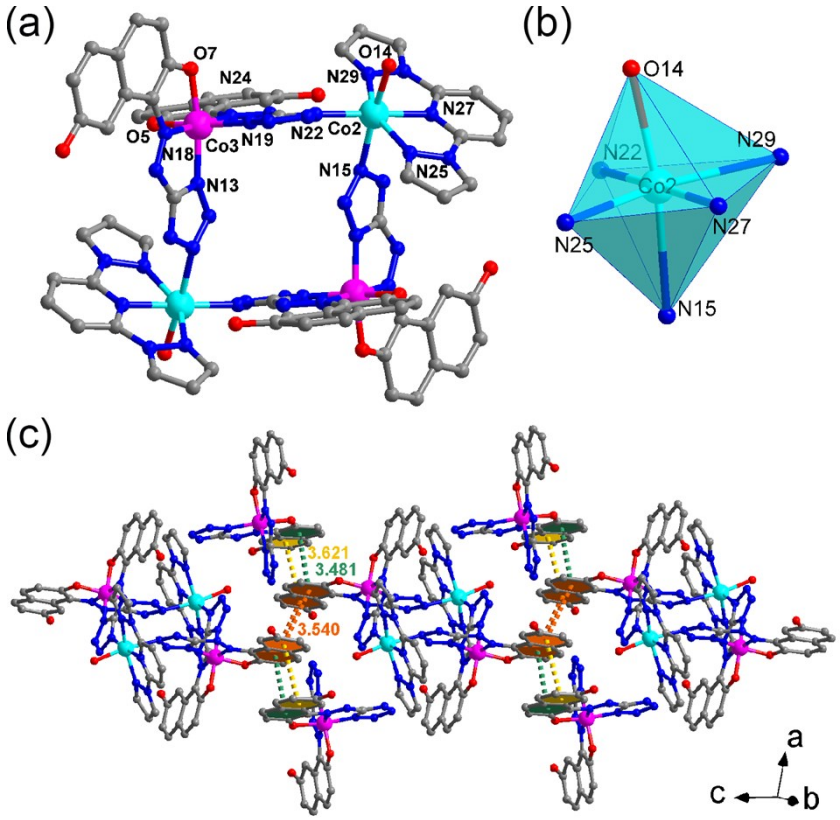

Fig. S4 Crystal structure of cation of complex **4** (a); Local coordination geometry of Co2 (b) and 1D structure through the π···π stacking interaction between naphthalene rings (c). Color code: pink, Co^{III}; turquoise, Co^{II}; gray, C; blue, N; red, O. Hydrogen atoms were omitted for clarity reason.

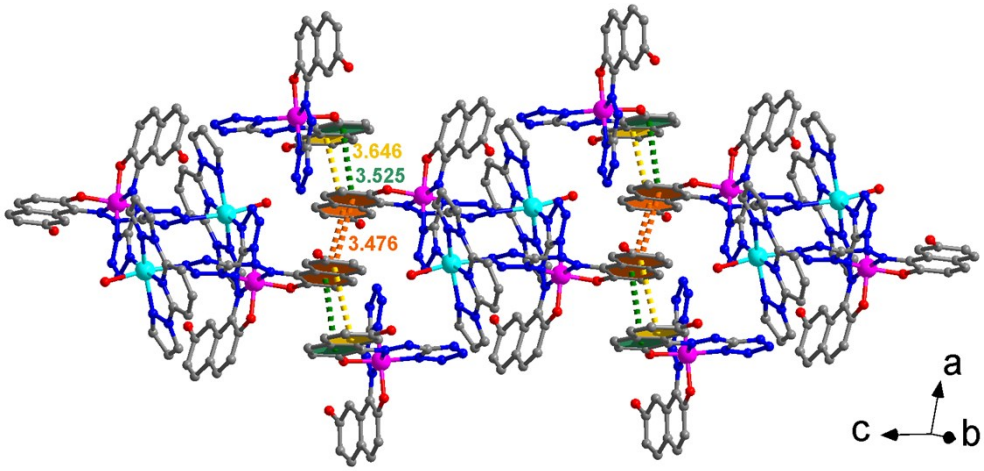

Fig. S5 1D structure through the π···π stacking interaction between naphthalene rings of complex **3**.

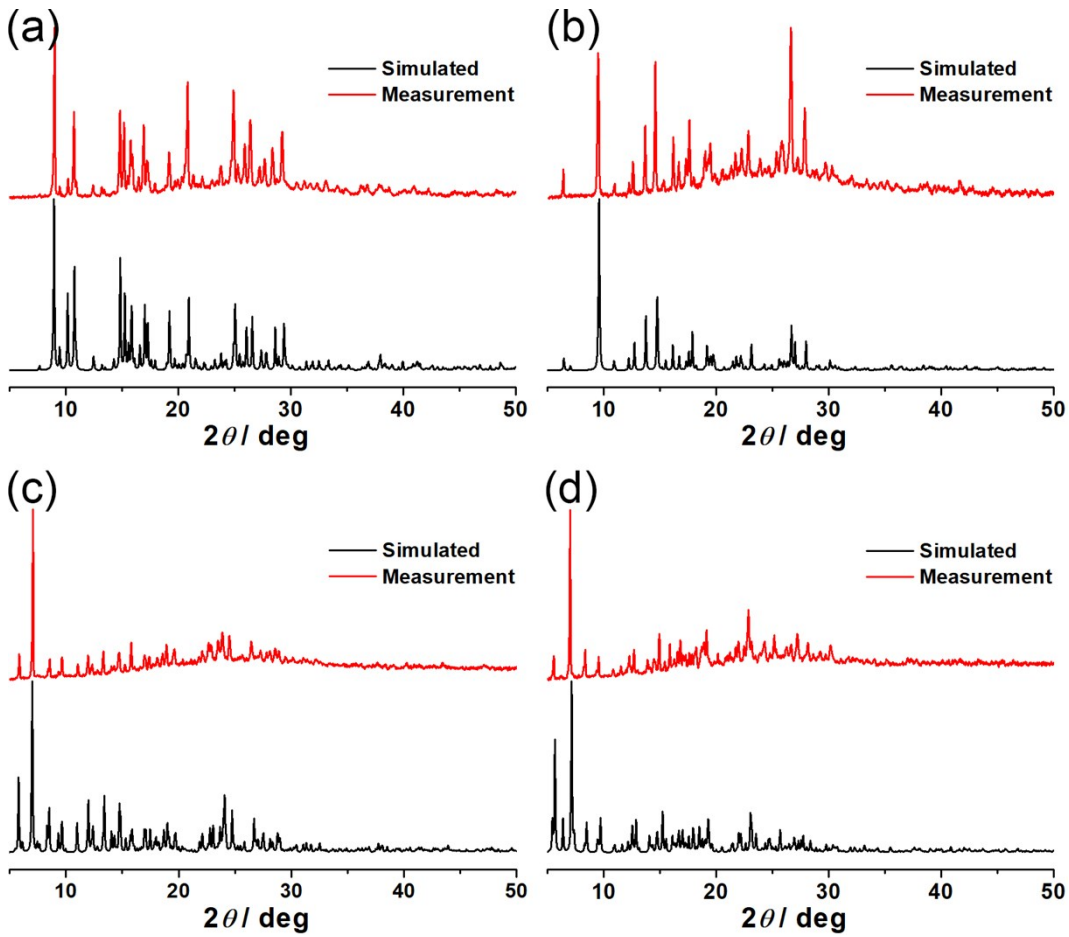

Fig. S6 Powder X-ray diffraction (PXRD) patterns for complexes **1**(a)**, 2**(b)**, 3**(c) and **4**(d)

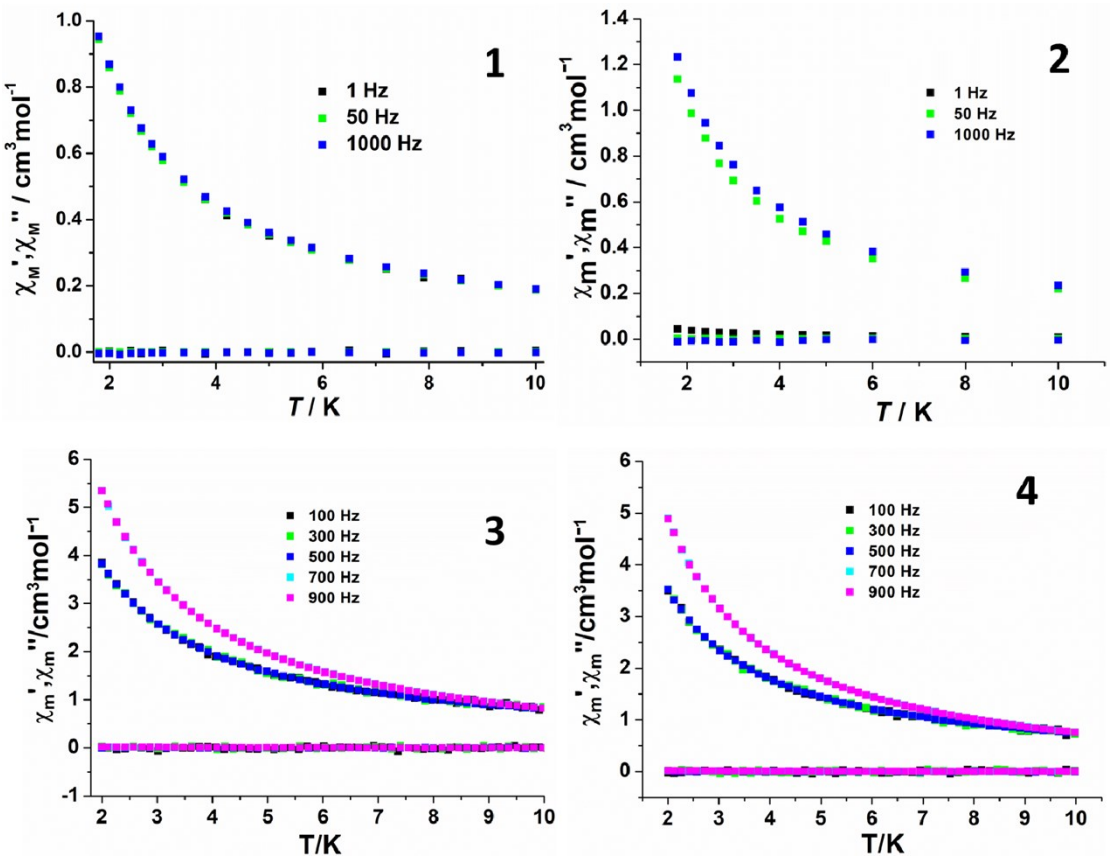

Fig. S7 Temperature dependence of the in-phase and out-of-phase for complexes **1**–**4** at zero DC-external field.

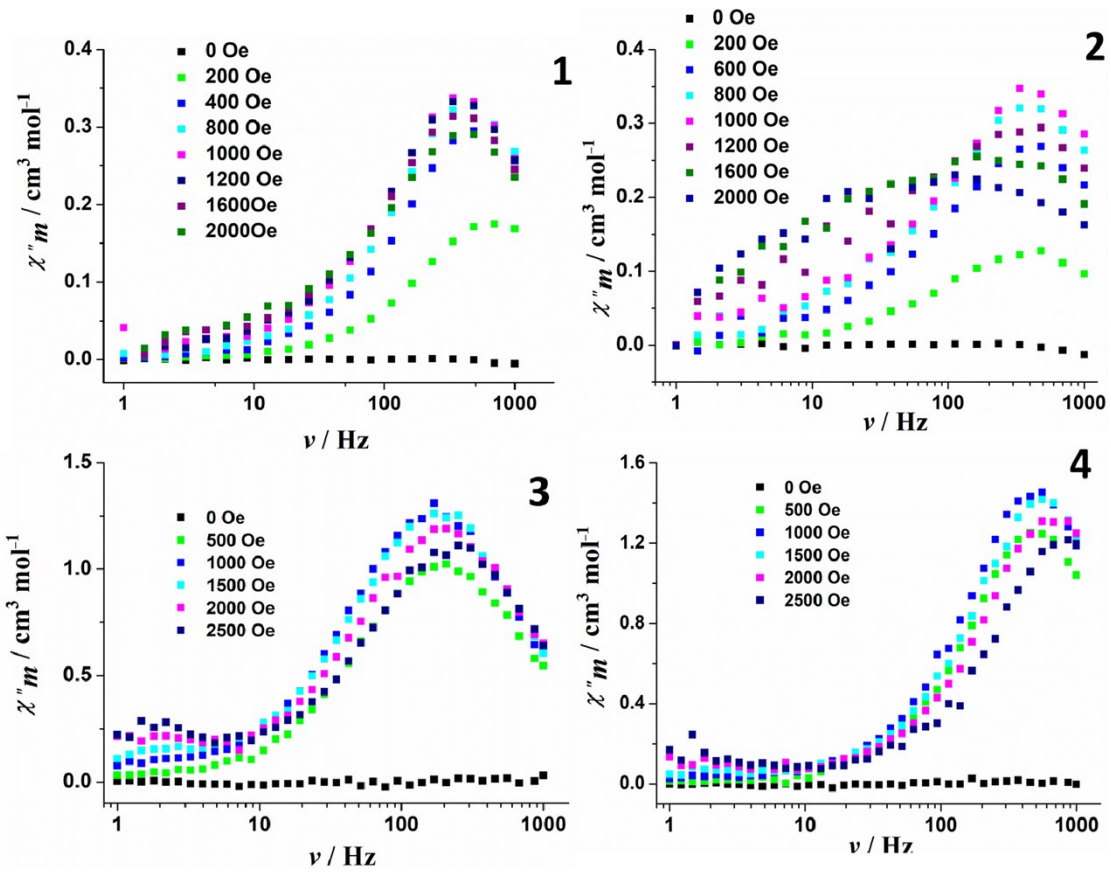

Fig. S8 AC susceptibility data for complexes **1**–**4** at 2 K under DC applied fields in the range 0-1000 Oe.

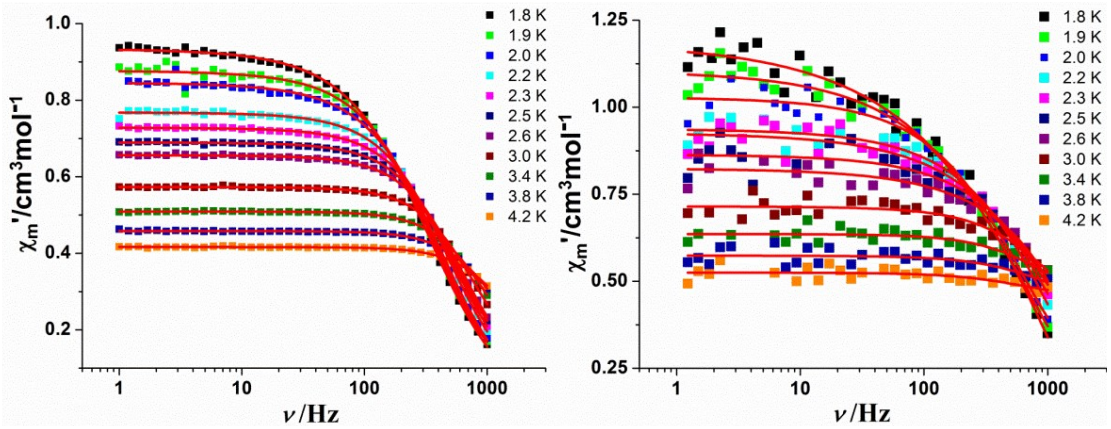

Fig. S9 Frequency dependence of the in-phase components for the ac magnetic susceptibility in a 1 kOe dc field for complexes **1** (left) and **2** (right). The solid lines represent the best fits with modified Debye functions (see the text).

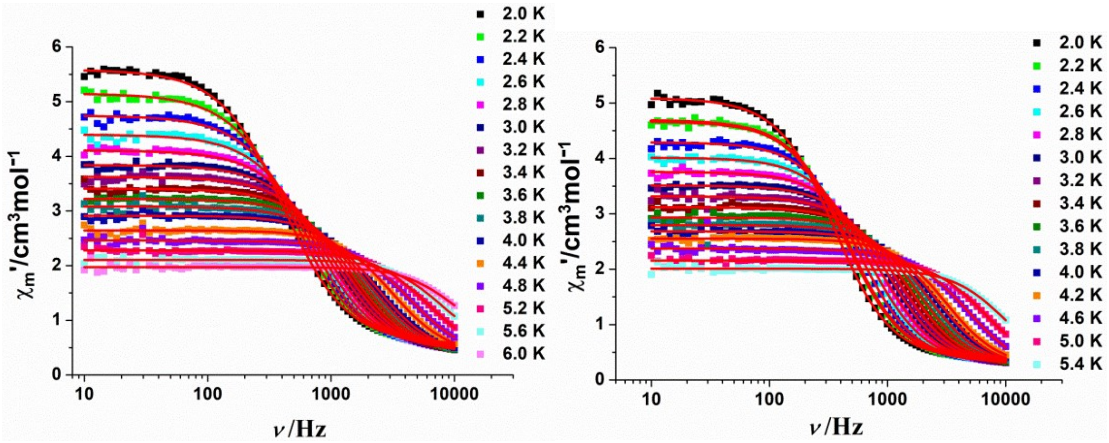

Fig. S10 Frequency dependence of the in-phase components for the ac magnetic susceptibility in a 1 kOe dc field for complexes **3** (left) and **4** (right). The solid lines represent the best fits with modified Debye functions (see the text).

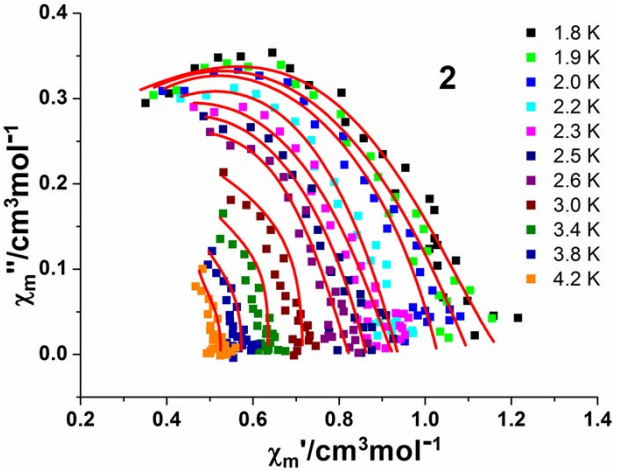

Fig. S11 Cole−Cole plots for complex **2**. The solid lines represent the best fits with modified Debye functions (see the text).

References

1 Brown, I. D., *IUCrJ*, 2017, **4**, 514-515.